Available online at www.sciencedirect.com
ScienceDirect
Thin Solid Films 515 (2007) 5804 – 5807
www.elsevier.com/locate/tsf

CdTe–CdS solar cells — Production in a new baseline and investigation of material properties

M. Hädrich *, N. Lorenz, H. Metzner, U. Reislöhner, S. Mack, M. Gossla, W. Witthuhn

Institut für Festkörperphysik, Friedrich-Schiller-Universität Jena, Max-Wien-Platz 1, 07743 Jena, Germany

Available online 25 January 2007

Abstract

In this paper, we describe our new baseline for CSS–CdTe–CdS solar cells on 10×10 cm^2 substrates. The deposition of the p–n junction and all the following steps were performed at the Institut für Festkörperphysik (IFK) in Jena. Using the new baseline, we are already able to produce solar cells with similar properties as commercial ones. In the batch type process, all manufacturing steps can be investigated separately. We employ Rutherford backscattering spectrometry (RBS), X-ray diffraction (XRD) and external quantum efficiency (EQE) measurements to characterise the structure of the bulk materials and interfaces. It is demonstrated that by RBS the front contact becomes accessible for thinned CdTe films. At the back contact, RBS spectra show a tellurium accumulation which is due to etching. This tellurium rich layer is confirmed by XRD with Rietveld refinement. The intermixing at the CdS–CdTe interface caused by the activation step is quantified by a bandgap determination based on EQE measurements. From the bandgap energy of the $CdTe_{1-x}S_x$ compound, we calculated the sulphur fraction x at the interface. XRD measurements imply that the activation step induces a (111) texture in CdTe. With regard to an improved manufacturing process, our cells are compared to industrial cells produced by Antec Solar Energy.

Keywords: Cadmium telluride CdTe; CdS; CdTe solar cells

1. Introduction

CdTe with a direct band gap of 1.45 eV is a very suitable absorber material for thin film solar cells. It grows p-type and highly stoichiometric forming a heterojunction with n-type CdS [1,2]. High AM1.5 conversion efficiencies of more than 16% for small area laboratory cells have been obtained using the close space sublimation (CSS) technique [3]. As the efficiencies of industrial modules with large areas are still less than 10%, improving CdTe thin film technology is essential [4]. We established a laboratory-scale baseline for the production of CSS–CdTe–CdS solar cells at the IFK to investigate and improve the manufacturing steps under close-to-industrial conditions. The translation of good cell performance to larger areas is aimed at by employing 10×10 cm^2 float glass substrates from the Antec production line.

2. Experimental

The glass substrates were already covered with ITO as transparent conducting oxide and SnO_2 as buffer layer from Antec. The deposition of first the CdS and then the CdTe layer was carried out in identical CSS chambers at a pressure of approximately 10^{-3} Pa. With substrate temperatures between 720 K and 770 K and source temperatures of up to 950 K, high growth rates of 50 nm/min to 100 nm/min for CdS and 2 μm/min to 8 μm /min for CdTe were reached. For solar cells, CdS layers of typically 100 nm and CdTe layers between 5 μm and 12 μm thickness were grown. The activation step was carried out either using a wet-chemical process or reactive annealing in gaseous HCl. For the wet-chemical treatment, the samples were covered with a solution of 0.2% to 1% $CdCl_2$ in methanol and annealed at 690 K in air. The gaseous HCl activation was performed in a quartz tube furnace with resistive heating at a pressure of 5×10^4 Pa and continuous gas flow. A gas mixture of 0.1% HCl in synthesized air and annealing temperatures of up to 670 K were used. For back contact formation, the samples were exposed to NP-etch solution (65% HNO_3, 85% H_3PO_4 and H_2O in a volume ratio of 1:70:29) for 60 s and afterwards rinsed in

* Corresponding author. Tel.: +49 3641947357; fax: +49 3641947302.
E-mail address: mathias.haedrich@uni-jena.de (M. Hädrich).

0040-6090/$ - see front matter © 2006 Elsevier B.V. All rights reserved.
doi:10.1016/j.tsf.2006.12.036

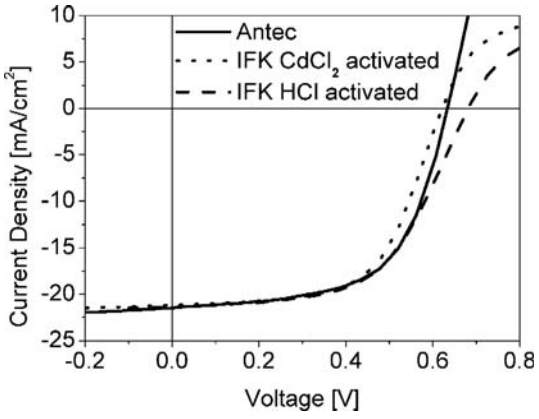

Fig. 1. Comparison of current–voltage characteristics of a typical cell from the Antec production line, a $CdCl_2$ activated IFK cell and an HCl activated IFK cell.

deionised water and dried with nitrogen gas. As metal back contact, molybdenum with a thickness of 750 nm was deposited by ion sputtering.

The sulphur amount at the CdTe–CdS interface for differently activated solar cells was determined based on a bandgap evaluation from EQE measurements. The bandgap energy is obtained from a $EQE^2(h\nu)^2$ versus $h\nu$ plot by extrapolating the linear part of the curve to the intersection with the $h\nu$ axis [5]. The dependence of the bandgap on the sulphur compound x is given by the empirical equation

$$E_G(x) = 2.4x + 1.51(1-x) - 1.8x(1-x) \quad (1)$$

Values of x between 0.2 and 0.8 cannot be reached for temperatures below 700 °C because of the miscibility gap in the phase diagram [6,4].

The chemical composition and thickness of the solar cell layers were analysed by Rutherford backscattering spectrometry (RBS). The experiments were carried out at the 3MV Tandetron Accelerator JULIA in Jena. For the measurements, 10 μC of 3.5 MeV He^{2+} ions were detected under a backscattering angle of 170°. RBS data were analysed using the computer code RUMP [7]. The samples for RBS measurements had a CdTe film thickness in the order of 1 μm and were covered with 200 nm of molybdenum.

3. Results and discussion

3.1. Solar cells

Using the baseline described above, we have produced solar cells with either wet-chemical or HCl activation. In Fig. 1, a comparison of an industrial cell from Antec with an HCl and a $CdCl_2$ activated IFK cell is shown. The three cells, all with an area of about 1 cm^2, have similar efficiencies, current densities and fill factors as shown in Table 1. The roll-over phenomenon is only present for the IFK cells which also have a higher series resistance. This implies that the back contact still needs to be improved. However, the HCl activated IFK cell yields the highest voltage of the compared cells and both IFK cells have a higher shunt resistance than the Antec cell.

Table 1
Comparison of solar cells from Antec and the IFK ($CdCl_2$ or HCl activation as indicated) in terms of series and shunt resistance R_S and R_{Shunt}, open circuit voltage V_{OC}, current density J_{SC}, fill factor FF and efficiency η

	R_S [Ω cm^2]	R_{Shunt} [Ω cm^2]	V_{OC} [mV]	J_{SC} [mA/cm^2]	FF	η [%]
Antec	5	335	637	21.7	0.59	8.2
IFK, $CdCl_2$	8	607	626	21.2	0.60	7.9
IFK, HCl	10	577	680	21.3	0.57	8.2

3.2. EQE

We investigated the activation step by EQE measurements. It is assumed that the activation leads to intermixing of CdS and CdTe at the interface which has been confirmed e.g. by XRD and PL measurements [8]. On the one hand this intermixing turns the abrupt junction into a continuous one and adjusts the lattice constants. On the other hand pinholes can occur in CdS [9]. We performed EQE measurements on IFK cells which were wet-chemically activated for different times, HCl activated IFK cells and already activated cells from Antec which were additionally subjected to a wet-chemical activation between 0 and 30 min. To quantify the intermixing, we determined the bandgap and sulphur fraction x in the $CdTe_{1-x}S_x$ compound. Both for the wet-chemically activated IFK cells and the Antec cells the bandgap decreases with longer activation time. In Fig. 2, it can be seen that the decrease in the bandgap is due to an increased sulphur fraction. For the 30 min additionally activated Antec cell, the sulphur fraction almost doubles from about 0.03 to nearly 0.06 which is approximately the solubility limit for an annealing temperature of 420 °C [6]. This is also visible in the EQE($h\nu$) plot where the steep descent at the bandgap energy of 2.4 eV for CdS softens with stronger activation meaning that the CdS layer becomes porous and is used up. In fact, both for Antec and IFK cells the shortest of the tested times for wet-chemical activation led to the highest efficiencies. The IFK cell activated with gaseous HCl yields the highest bandgap

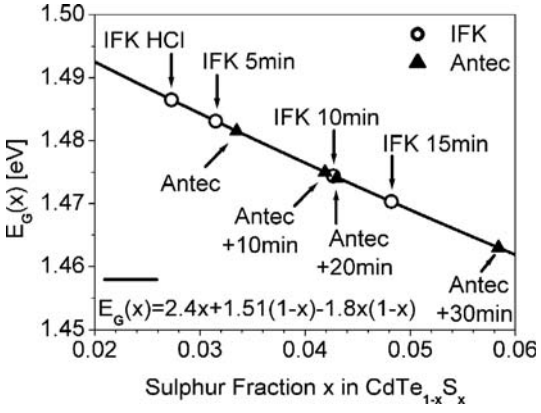

Fig. 2. Bandgap curve of $CdTe_{1-x}S_x$ as a function of the sulphur fraction x according to Eq. (1) with inserted bandgap data points of IFK cells with different times of wet-chemical activation, an HCl activated IFK cell, an Antec cell and Antec cells with different times of additional activation. The activation times are as indicated at the data points.

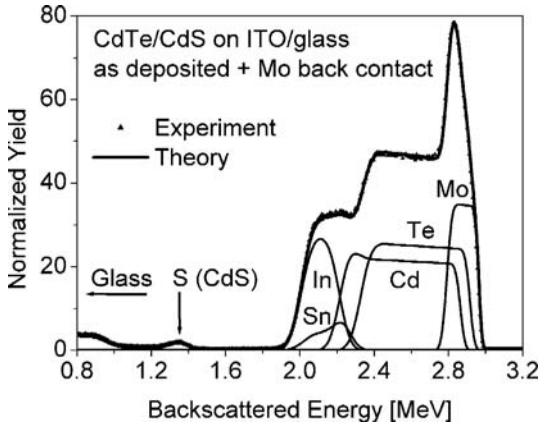

Fig. 3. RBS spectrum of a molybdenum covered, as deposited CdTe/CdS layer system on ITO/glass substrate.

and smallest sulphur fraction of the compared cells indicating that this type of activation leads to the least intermixing.

3.3. RBS

It has been shown that RBS is a useful tool to investigate CdS–CdTe bilayers in terms of sulphur diffusion after activation [10]. We used RBS to investigate the influence of the etching step on the back contact. In Fig. 3, an RBS spectrum of a Mo–CdTe–CdS–TCO-glass structure is shown. For the thin CdTe films (≤1.5 μm) we analysed, the thickness and composition of all front contact layers beneath are accessible to the measurement. By fitting the data by a theory curve, the layers are identified to be 200 nm Mo, 1 μm CdTe, 100 nm CdS, 45 nm SnO_2 and 470 nm ITO. The values for Mo, CdTe and CdS are in good accordance with profilometric thickness measurements of single layers. The glass substrate has an infinite thickness for the measurement. The spectrum shown in Fig. 4 was measured for an equal Mo–CdTe–CdS–TCO-glass structure, however the CdTe layer was NP-etched prior to back contact deposition. A pronounced change of the backscattered yield at the high energy edge of CdTe is visible which can only be explained when a strong Te peak is assumed. That corresponds to a Te rich layer at the surface of CdTe. NP-etched CdTe surfaces are known to contain TeO_x phases. XPS measurements revealed oxygen fractions in the order of 20% [11,12]. We had to assume 30% of oxygen in the Te rich layer for the RBS fit. Oxygen as a light element is not directly visible in the spectrum, however it reduces the yield of the Te peak. The simulation of the measured curve is also possible without assuming oxygen but leads to a Te peak which lies 4% above the measured curve. This deviation might also be due to a porous Te layer, as suggested elsewhere [13]. Whether the layer is

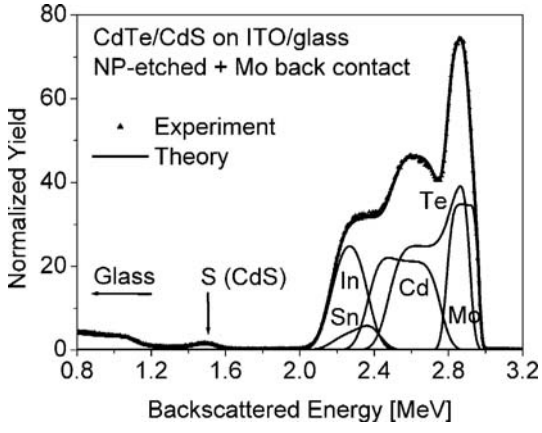

Fig. 4. RBS spectrum of a molybdenum covered, NP-etched CdTe/CdS layer system on ITO/glass substrate.

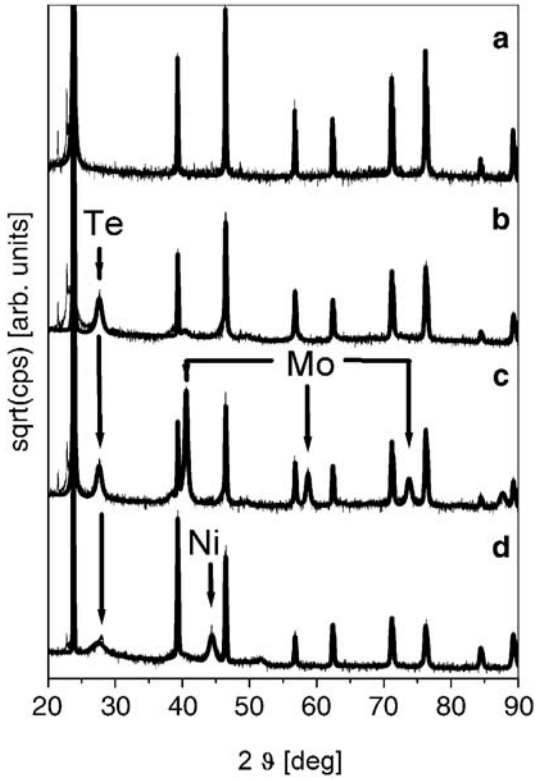

Fig. 5. XRD spectra of: a)–c) a solar cell from the Antec production line: a) without back contact, b) NP-etched at IFK, c) with IFK molybdenum back contact and d) an Antec solar cell with nickel back contact.

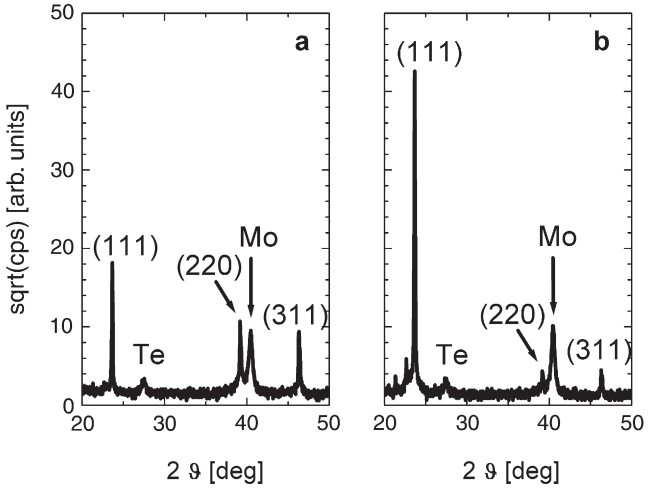

Fig. 6. XRD spectra of CdTe–CdS solar cells: a) not activated, b) activated.

oxidized or porous cannot be decided from RBS spectra. According to the RBS evaluation, the Te layer thickness is about 250 nm. Different values of several 100 nm [11,12] or 10 nm [13] respectively have been reported. The Te layer thickness might depend on the morphology of CdTe, e.g. because of preferential etching at the grain boundaries. As a thick Te layer might strongly affect the conduction, further investigations are necessary.

3.4. XRD

The appearance of a Te enriched layer at the surface of CdTe after etching was also investigated by XRD. In Fig. 5, XRD spectra for a) an Antec CdTe layer, b) this layer after NP-etching at IFK and c) the etched layer with molybdenum back contact made at IFK are shown. The spectrum of a solar cell structure completely processed by Antec is shown in Fig. 5d. Both for Antec and IFK cells, the Te peak after etching is clearly visible, although for the latter it is more pronounced. The reason might be that for Antec cells a Sb_2Te_3 layer is used as diffusion barrier to the nickel back contact. However, it is also possible that the etching step at IFK leads to a thicker Te layer which would agree with the RBS results described above. XRD spectra also revealed significant differences of CdTe texture between a not activated (Fig. 6a) and an activated (Fig. 6b) IFK cell. The strong increase of the (111) CdTe peak after activation indicates a recrystallisation from nearly random grain orientation to a pronounced (111) texture. A similar behaviour was observed for Antec cells. The effect of the activation on the morphology of CdTe depends amongst others on the CdTe deposition method [14]. For CSS deposited films, the induction of a CdTe (111) texture which increases with higher $CdCl_2$ concentration has been reported [9]. For layers deposited by high vacuum evaporation on the other hand, a loss of the former (111) texture was found which was complete for low and partial for high activation temperatures [14].

4. Conclusion

With the baseline described above, we are able to produce CSS–CdTe–CdS solar cells with similar properties as commercial cells from Antec. The activation step induces a (111) texture for both kinds of cells. Furthermore a $CdTe_{1-x}S_x$ phase is formed at the interface whereas the sulphur fraction rises with the activation time and is between 0.03 and 0.06. Of the compared cells, the ones with the smallest sulphur fractions also showed the best performance. In RBS measurements of solar cells with a CdTe film thickness of about 1 μm, the complete layer system including the front contact can be investigated. The formation of a tellurium rich layer after etching is visible both in XRD and RBS spectra.

Acknowledgements

We thank the Bundesministerium für Umwelt, Naturschutz und Reaktorsicherheit for funding this work (Förderkennzeichen 0329881). We thank Antec Solar Energy for supplying production material and commercial samples.

References

[1] D. Bonnet, P. Meyers, J. Mater. Res. 13 (1998) 2740.
[2] D. Bonnet, Thin Solid Films 361–362 (2000) 547.
[3] X. Wu, J.C. Keane, R.G. Dhere, C. DeHart, D.S. Albin, A. Duda, T.A. Gessert, S. Asher, D.H. Levi, P. Sheldon, Proceedings of the 17th European Photovoltaic Solar Energy Conference, Munich, Germany October 22–26, 2001, p. 995.
[4] B.E. McCandless, J.R. Sites, in: A. Luque, S.S. Hegedus (Eds.), "Cadmium Telluride Solar Cells", Handbook of Photovoltaic Science and Engineering, Wiley and Sons, Chichester, 2003, p. 617.
[5] J. Kessler, D. Schmid, R. Schäffler, H.W. Schock, S. Menezes, Conf. Rec. 23 rd IEEE Photov. Spec. Conf. IEEE, New York, 1993, p. 549.
[6] G. Jensen, Alloys in Cadmium Telluride Solar Cells, Stanford University, 1997.
[7] L.R. Doolittle, Nucl. Instrum. Methods Phys. Res., B 15 (1986) 227.
[8] M.H. Aslan, W. Song, J. Tang, D. Mao, R.T. Collins, D.H. Levi, R.K. Ahrenkiel, S.C. Lindstrom, M.B. Johnson, Mat. Res. Soc. Symp. Proc., vol. 485, AIP Press, 1998, p. 203.
[9] P.D. Paulson, V. Dutta, Thin Solid Films 370 (2000) 299.
[10] D. Grecu, A.D. Compaan, J. Appl. Phys. 87 (2000) 1722.
[11] J. Sarlund, M. Ritala, M. Leskelä, E. Siponmaa, R. Zilliacus, Sol. Energy Mater. Sol. Cells 44 (1996) 177.
[12] D.W. Niles, X. Li, P. Sheldon, H. Höchst, J. Appl. Phys. 77 (1995) 4489.
[13] D. Kraft, A. Thissen, J. Broetz, S. Flege, M. Campo, A. Klein, W. Jaegermann, J. Appl. Phys. 94 (2003) 3589.
[14] A. Romeo, D.L. Bätzner, H. Zogg, A.N. Tiwari, Thin Solid Films 361–362 (2000) 420.